Eur. Phys. J. B **47**, 319–328 (2005)
DOI: 10.1140/epjb/e2005-00325-x

THE EUROPEAN PHYSICAL JOURNAL B

Statistical analysis of floating-car data: an empirical study

M.E. Fouladvand[1,2] and A.H. Darooneh[1,3,a]

[1] Department of Physics, Zanjan University, P.O. Box 45196-313, Zanjan, Iran
[2] Department of Nano-Science, Institute for Studies in Theoretical Physics and Mathematics (IPM), P.O. Box 19395-5531, Tehran, Iran
[3] Sufi Institute, P.O. Box 45195-1547, Zanjan, Iran

Received 20 April 2005 / Received in final form 6 July 2005
Published online 11 October 2005 –

Abstract. We present the results of statistical analysis of the empirical floating-car data. Our investigations are based on analyzing the time series of four basic quantities namely velocity, velocity difference, spatial gap and the acceleration associated to some instrumented cars. We obtain the statistical characteristics, including the mean, variance and relative variance of these time series by taking direct time averages. We also try to identify the moving phases of the instrumented vehicle according to the statistical properties of its velocity time series. Moreover, by exploring the two-point joint probabilities, we propose a new approach for modelling vehicular dynamics based on the floating car data.

PACS. 45.70.Vn Granular models of complex systems; traffic flow – 05.90.+m Other topics in statistical physics, thermodynamics, and nonlinear dynamical systems – 05.10.-a Computational methods in statistical physics and nonlinear dynamics

1 Introduction

Empirical observations on spatial-temporal structure of traffic flow have revealed inherent complexities both on microscopic and macroscopic levels [1–12]. The early traffic models were only able to reproduce only a few basic features of realistic traffic flow the most important of which was the formation of spontaneous jams. Nevertheless, almost all these models (for a detailed review, refer to reviews [4,5]) failed to reproduce the microscopic organisation of traffic flow. Technically speaking, non of these models could predict three identified phases of traffic flow. This was mainly due to simple treatment of car-car interactions and unrealistic implementation of acceleration/deceleration. Quite recently significant endeavors has been accelerated towards the thorough understanding of traffic flow dynamics by introducing several improvements to the preexisting models [13–19]. Among the recent models, only a few of them are capable of reproducing the three phases of traffic flow the so-called *free, synchronized* and *wide moving jams* [15–17]. Even these model can not fully reproduce the microscopic structures of traffic flow specially in relatively congested situations. Inevitably, in order to compare the microscopic single-vehicle predictions of each model to reality, one has to know the empirical behaviours of typical cars in different traffic states. So far the empirical data were mainly gathered via induction loop installed at fixed locations of the road. With the help of these loops we can, in principle, measure the averaged velocity, flux, density (occupancy) at the position of the detector. In this way one obtains local information about the flow. Although one achieves useful information about the flow, this scheme is inadequate to provide the necessary information about the long time behaviour of individual cars. In order to get insight into the real-life driving behaviour of individual drivers, one should be able to have a time record of individual cars. Principally, these types of data can be obtained by instrumentation of a car with lidar/radar detectors. These detectors can simultaneously measure the velocity and the acceleration of the instrumented car, velocity of its leader and the spatial gap to its leader. This floating-car data can be used to test the validity or the development of more sophisticated models of vehicular movement. Very recently a novel approach to modelling traffic flow based on empirical floating car data has been introduced [20]. In this approach, the empirical distribution of temporal headway has been taken into account to develop a Langevin-type formulation for the equations of velocity and the position of cars. It is our major objective in this paper to report on a detailed statistical analysis of empirical floating car time series of four basic quantities i.e., velocity , velocity difference, spatial gap and acceleration/deceleration. On the account of this analysis, we try to classify the driving states of the floating car. This can give useful information about the traffic state in the environment of the floating car. Besides, we try to introduce a new approach for treating the car-car

[a] e-mail: `darooneh@mail.znu.ac.ir`

interaction on a more realistic grounds. The organisation of this paper is as follows. In section one, we motivate the problem and introduce some preliminary mathematical tools needed for our statistical analysis. Sections two and three contain the results obtained from the empirical floating-car measurements. In section four we discuss one and two-point distribution functions and that how the floating car data can be implemented for making new models and parameter calibration of existing models. Conclusions and summaries are given in section five.

2 Time series analysis of floating-car data

While from the viewpoint of individual drivers, the driving strategy is deterministic, the heterogeneous behaviours of multitude of drivers make the traffic flow appear as a complex many body interacting systems. Diversity of individual drivers' behaviour and the types of their responses to various traffic stimuli received from their environment such as fluctuations of their leader vehicles, hindrances, road conditions etc together with mental effects allows us to assume traffic flow as a random process. If we look at the velocity record of a typical vehicle during a finite time interval, we would certainly realize that this velocity, $v(t)$, is a seemingly erratic and fluctuating function of time and its statistical properties depend on the global traffic congestion around the vehicle. Similar arguments correspond to the other single-vehicle quantities such as the spatial gap, or headway as is often called, to the leader vehicle $g(t)$, the vehicle acceleration $a(t)$ and the velocity difference $\Delta v(t) = v_l(t) - v(t)$ to its leader vehicle ($v_l(t)$ denotes the leader's velocity). It is our objective in this paper to introduce some characteristic aggregate statistical functions which give us a better insight to the stochastic aspects of traffic flow and enables us to establish a more realistic modelling framework of the driving rules and strategies. The fundamental quantity to deal with is each particle (vehicle) velocity. Other physical quantities are derived from the velocity. To be more explicit, let us associate some variables (physical quantities) $X_k \quad k = 1, 2, 3 \cdots$, to each vehicle driving in a road. We label each car by a number i and specify the kth variable related to the ith car by the X_k^i respectively. For both practical purposes and modelling objectives, we let time elapses in discrete steps denoted by $\delta t = \tau$ and specify the value of variable X_k^i at the end of n-th time step $t = n\tau$ by $X_k^i(n)$. We now define the time average of X_k^i over a real time period of duration T time steps starting from step $n = n_1$ until step $n = n_2 = n_1 + T$ as follows:

$$\overline{X_k^i(n_1, T)} = \frac{1}{T} \sum_{n=n_1}^{n_1+T} X_k^i(n). \tag{1}$$

We should emphasize that due to non-stationary aspect of the time series, the value of the averaged quantities will, in general, depend on the starting time step n_1. We now proceed by considering the temporal auto and cross correlations. Temporal auto-correlation function of variable X is defined as follows:

$$A_X(\tau, n_1, T) = \frac{1}{T-\tau} \sum_{n=n_1}^{n_1+T-\tau} X(n)X(n+\tau). \tag{2}$$

Having defined the temporal autocorrelation function, one can introduce a normalized auto correlator as follows:

$$\rho_X(\tau, T) = \frac{A_X(\tau, n_1, T) - \overline{X}(n_1, T)\overline{X}(n_1+\tau, T-\tau)}{\sigma_X(n_1, T)\sigma_X(n_1+\tau, T-\tau)} \tag{3}$$

with $\sigma_X(n_1, T) = \overline{X^2(n_1, T)} - \overline{X(n_1, T)}^2$.

It can be shown that normalized auto-correlation satisfies the inequality: $-1 \leq \rho_X(\tau, n_1, T) \leq +1$ for all τ, n_1 and T. By virtue of the above argument, one can define cross-correlation functions of variables X and Y denoted by $C_{X,Y}(\tau, n, T)$ by simply replacing the second X in the above formula with the associated Y variable. To deal in some depth, we shall now focus on the velocity of a particular vehicle say i. In empirical measurements, time is measured in discrete multiples of τ and the position of each vehicle is recorded as the multiple of a space grid denoted by δx. The time and space discretisation induces a discretisation for the velocity denoted by δv which is given by $\delta v = \delta x/\tau$. Regarding this fact, the integer-valued velocity ranges from 0 to $v_{max} = n_{max}\delta v$. By this notion, the velocity time series gives rises to the integer-valued velocity distribution function denoted by $P^i(v; \delta v, T)$. It is the relative frequency of the integer velocity v of the i-th vehicle during the period $[n_1\tau, n_2\tau]$. Now we consider the joint distribution functions. For simplicity let us consider the two-point function and take $X_1 = v$ and $X_2 = g$. In this case $P_2^i(v, g)$ is the relative frequency of time steps (during the measurement time interval T) at which the velocity and the gap of the i-th vehicle takes the integers v, g respectively. Note that for notational convenience, we have not explicitly written δv and T in the argument of $P_2^i(v, g)$. Higher N-point functions can analogously be constructed.

3 Empirical results

In this section we obtain some of the distribution functions in the above sections. We recall that most of the present data in the literature has been gathered through loop detectors at various points of the road [11,12,21–26]. We do not intend to discuss these types of data. The readers can refer to review articles and related papers in the field [4,5,9,10,12,21–23,25,26]. There are basic differences between floating-car data and those obtained from fixed loop detectors. Each of these types of data give their own useful information. Specifically, fixed detectors measure the local properties of traffic flow, namely flow, occupancy, average velocity etc, at certain locations of the road. However, they cannot give us illustrative information about the individual cars behaviour unless lots of detectors are installed which seems infeasible. On the other hand, to gain significant insight into the vehicular dynamics, it is salient to analyse the car-car interaction. Fixed detectors are inadequate and unable to provide enough information for such vital analysis. Therefore, having floating-car data seems unavoidable [27–29]. Recently there has been an increasing attempt to gather floating vehicle date mainly in order to calibrate the parameters needed for the modelling of vehicular dynamics in the framework of car-following models [20,31–34]. These are among the basic reasons why there are couple of projects running world wide to gather trajectory data. In this paper we intend to report on the analysis of empirical data taken from some floating cars. The data we have analysed have been gathered from some equipped cars on German highways [30]. They contain time series of v, Δv, g and a. These four quantities have been recorded at 0.1 s intervals. The leader velocity is measured with radar while the follower velocity is measured by lidar technique. The number data in each figure is ten times the duration of measurement. The precision of acceleration is 0.125 m/s^2. Let us begin by showing the time series of v, Δv, g and a. The following sets of figures exhibit the time series of above-mentioned quantities for different driving situations. We have analysed the statistical properties of these time series by taking direct time averaging. We have calculated average, standard deviation and relative deviation (denoted by s) which is defined as the standard deviation divided by average provided that the average is non zero. Based on their statistical properties, four relatively different driving states have been identified. We call them fast (F), relatively fast (RF), slow (S) and very slow (VS) states. The discrimination is mainly due to the average value of the velocity and its fluctuation. However the type of correlation/anticorrelation among the four quantities constitute the other sources for identifying the states. Figure 1 considers the fast driving state. Generally speaking, the relative deviations are small. We have evaluated the temporal auto correlation of $v, \Delta v$ and g. All of them are weakly correlated over time scales up to 10 s and anti correlated for τ greater than 10 s. As can be seen from the graphs (and confirmed by mathematics) there is strong anti-correlation between velocity and the velocity difference to the leader up to 10 s. Between velocity and the gap, One observes a weak short correlation up to 3 s and a strong anti correlation between 4 s and 20 s. Between g and Δv we observe a rather strong correlation up to 20 s. Next (Fig. 2) we consider a relatively fast driving state. The driving behaviour can be inferred by looking at the velocity time series.

In comparison to the fast driving time series, one observes that fluctuations are enhanced. The average velocity of the car has reduced to 28 m/s. The range of velocity is wider and includes 22 to 32 m/s. The velocity standard deviation has notably increased to 2.56 m/s. Consequently the velocity relative deviation has sharply increased. Concerning the velocity difference, both the average, and its standard deviation have increased. For the gap, both standard and relative deviations have increased. auto correlation analysis shows that the velocity is correlated up to 18 s while Δv and g are more correlated (up to 30 s). v and g are correlated up to 6 s and uncorrelated after 6 s. Similar arguments apply to the case of v and Δv. Concerning the velocity difference and the gap, they are weakly correlated up to 5 s and then become uncorrelated ($\tau > 5$ s). Figure 3 exhibits the floating car behaviour in a slower driving state. As observed, the average velocity is further reduced to 19 m/s. This may corresponds to moving in a higher congested environment.

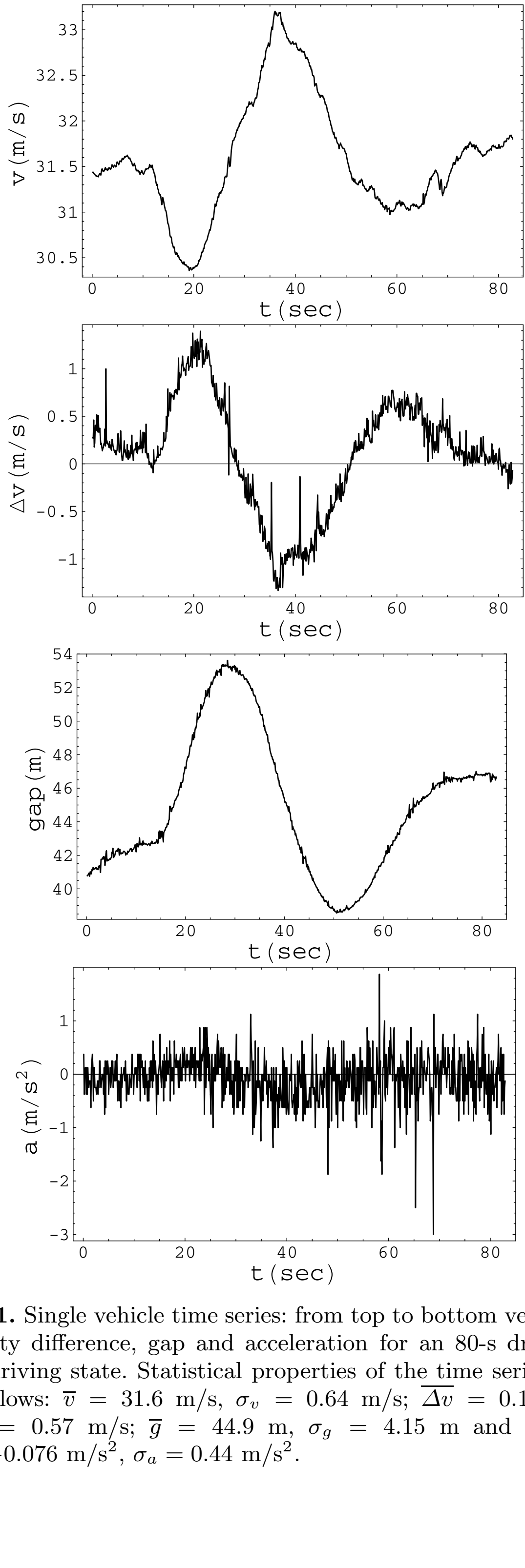

Fig. 1. Single vehicle time series: from top to bottom velocity, velocity difference, gap and acceleration for an 80-s drive in fast driving state. Statistical properties of the time series are as follows: $\overline{v} = 31.6$ m/s, $\sigma_v = 0.64$ m/s; $\overline{\Delta v} = 0.1$ m/s, $\sigma_{\Delta v} = 0.57$ m/s; $\overline{g} = 44.9$ m, $\sigma_g = 4.15$ m and finally $\overline{a} = -0.076$ m/s^2, $\sigma_a = 0.44$ m/s^2.

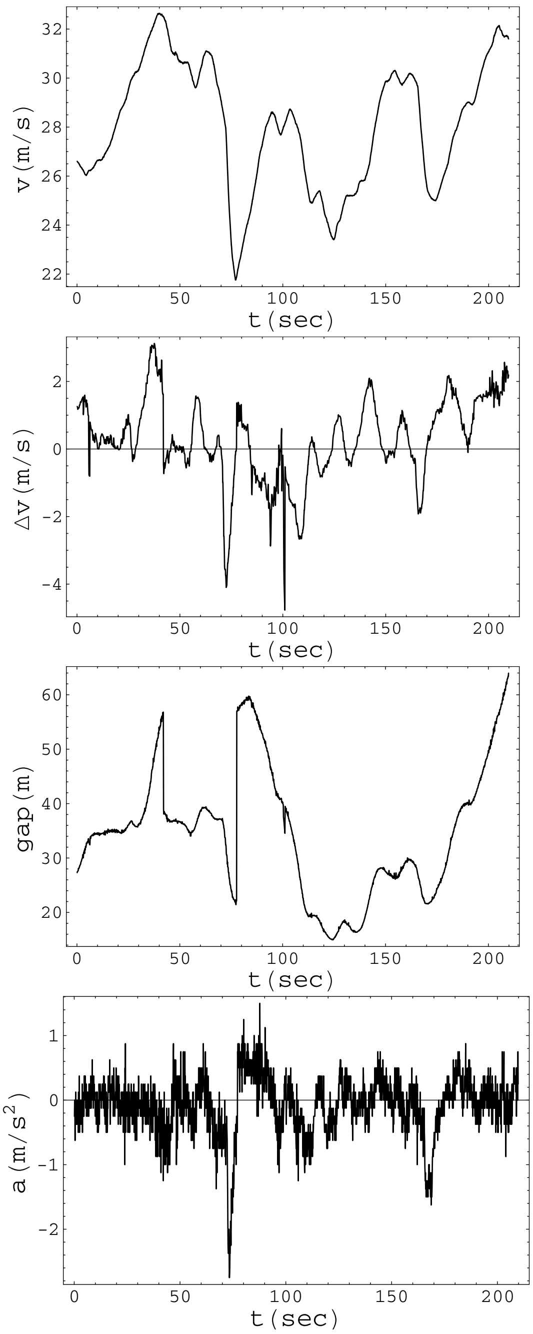

Fig. 2. Single vehicle time series: from top to bottom velocity, velocity difference, gap and acceleration for a 200-s drive in a relatively fast driving state. The statistical properties are as follows: $\overline{v} = 28.1$ m/s, $\sigma_v = 2.56$ m/s; $\overline{\Delta v} = 0.27$ m/s, $\sigma_{\Delta v} = 1.21$ m/s; $\overline{g} = 34.5$ m, $\sigma_g = 11.7$ m and finally those for the acceleration: $\overline{a} = -0.09$ m/s^2, $\sigma_a = 0.46$.

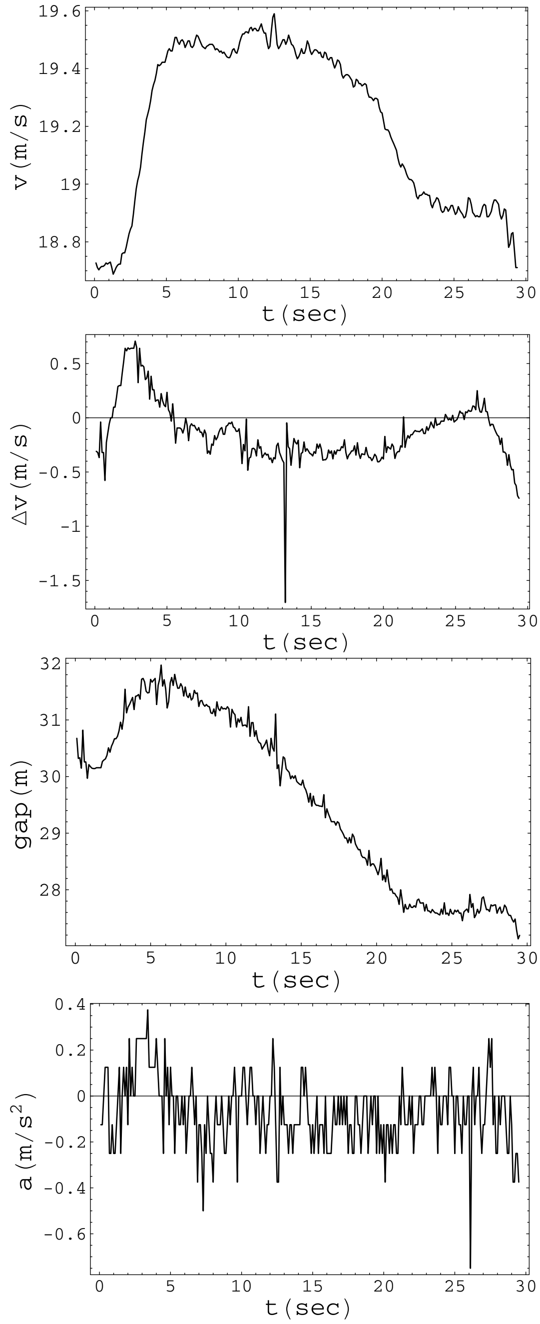

Fig. 3. Single vehicle time series: from top to bottom velocity, velocity difference, gap and acceleration for an 30-s drive in a slow driving state. The statistical properties are as follows: $\overline{v} = 19.2$ m/s, $\sigma_v = 0.28$ m/s; $\overline{\Delta v} = -0.13$ m/s, $\sigma_{\Delta v} = 0.27$ m/s; $\overline{g} = 29$ m, $\sigma_g = 1.5$ m and finally $\overline{a} = -0.07$ m/s^2, $\sigma_a = 0.15$ m/s^2.

Compared to Figure 2 velocity standard and relative deviations have notably reduced. However the velocity difference turns out to be more erratic since its standard deviation has increased in comparison to Figure 2. Furthermore, the gap's fluctuations is suppressed. Besides the value of the average velocity, a distinctive feature to the time series of Figure 2 is the reduction of the velocity standard deviation. This may be related to a high degree of synchronization of the vehicle's velocity to its leader's velocity. Since the driving interval is not long enough, the auto and cross correlations do not give rise to meaningful results. The next set of figures (Fig. 4) exhibits the floating car behaviour in a very much slow driving situation.

Although the average velocity is very small, the velocity standard deviation is relatively very large leading to

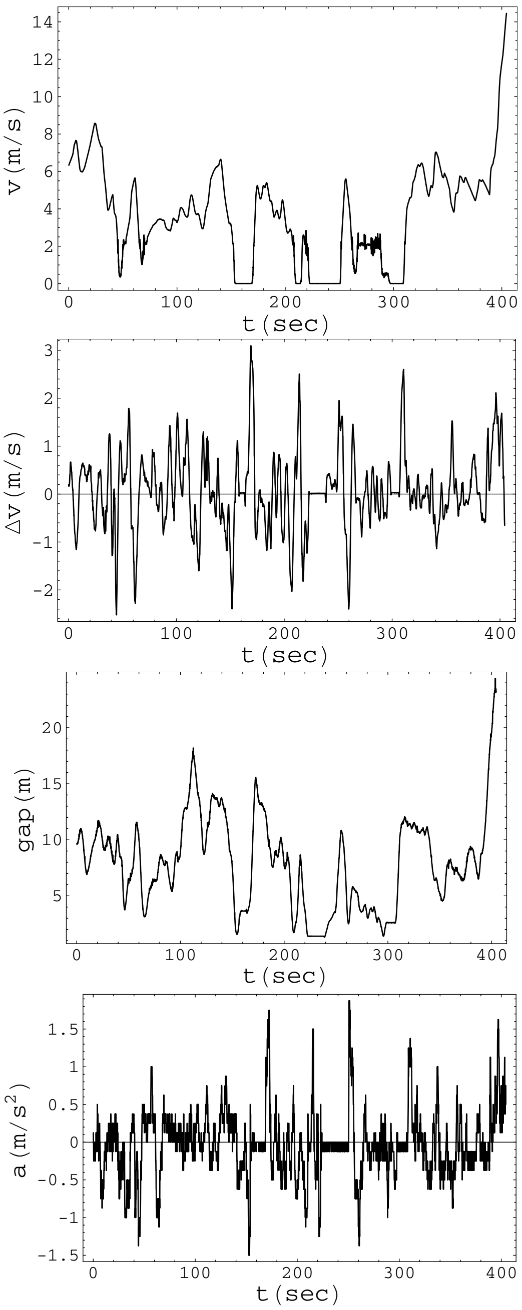

Fig. 4. Single vehicle time series: from top to bottom velocity, velocity difference, gap and acceleration for an 400-s drive in a very slow driving state. The statistical properties are as follows: $\overline{v} = 3.7$ m/s, $\sigma_v = 2.5$ m/s; $\overline{\Delta v} = 0.06$ m/s, $\sigma_{\Delta v} = 0.8$ m/s; $\overline{g} = 7.8$ m, $\sigma_g = 4.1$ m and finally $\overline{a} = -0.03$ m/s^2, $\sigma_a = 0.44 m/s^2$.

a large velocity relative deviation. In comparison to Figure 3, the velocity standard deviation has a considerable larger value. Concerning velocity difference, the average value is nearly zero but its standard deviation is larger than the value in Figure 3. Finally while the average gap has decreased to eight metres, the gap standard deviation is relatively high. The very slow state has the highest gap relative deviation among the times series discussed so far.

Table 1. Statistical properties of different drivingstates.

traffic state →	F	RF	S	VS
$\overline{v}$ (m/s)	31.6	28	19	3.7
σ_v (m/s)	0.64	2.56	0.28	0.8
$\overline{\Delta v}$ (m/s)	0.1	0.27	−0.13	0.06
$\sigma_{\Delta v}$ (m/s)	0.57	1.21	0.27	0.8
$\overline{g}$ (m)	45	34	29	8
σ_g (m/s)	4	11	1.5	4

v and g are correlated up to 20 s. In sharp contrast, Δv is correlated only over short time scales up to 3–4 s. Concerning the cross correlations, there is correlation between v and g up to 100 s. v and Δv are nearly uncorrelated. Between Δv and g one observes a fluctuating cross correlation between negative and positive values. We have summarized the statistical properties of the above time series denoted by fast (F), relatively fast (RF), slow (S) and very slow(VS) in the following tables.

Before closing this section, it would be illustrative to to clarify some points about the different driving states introduced above. The above classification can only be regarded as a preliminary naive one. While the average velocity serves to distinguish these states, there exists somewhat a degree of arbitrariness hence it is by no means a decisive criterion for driving state discrimination. Although we have tried to imply other statistical properties, such as correlation functions, our classification is not yet a rigorous one. Deeper analysis of further floating-car data that include driving behaviours in all the traffic situations will shed more lights upon this problem.

4 Distribution functions

We next derive the corresponding distribution functions from the above time series as explained in the preceding sections. In Figures 5–7 the related one-point distribution functions $P(v), P(g)$ and $P(\Delta v)$ are obtained. In obtaining the following distributions, the value of grids are as follows: velocity grid = 1 m/s, velocity difference grid = 0.25 m/s, gap grid = 1 m and acceleration/deceleration grid = 0.1 m/s^2. The number of data is 800 (F), 2000 (RF), 300 (S) and 4000 (VS) respectively. The number of data points in each bin can simply be evaluated by multiplying the bin's height at the data number of the corresponding driving state.

One can observe that in RF and VS states, the velocity distribution $P(v)$ is wide while it is localised in F and S states. For $P(\Delta v)$ this kind of behaviour is more or less the same. When coming to $P(g)$, the localized character is notably reduced in F state. In the RF state, except acceleration, all the other distribution functions widen (compared to free flow) which reflects the amplification of fluctuations. It should be noted that if we change the grid, the range of the distribution will remain unchanged while the form may undergo changes. By looking at the S and RF states, one infers a distinctive feature between them. In the latter, the distributions cover the narrow region of

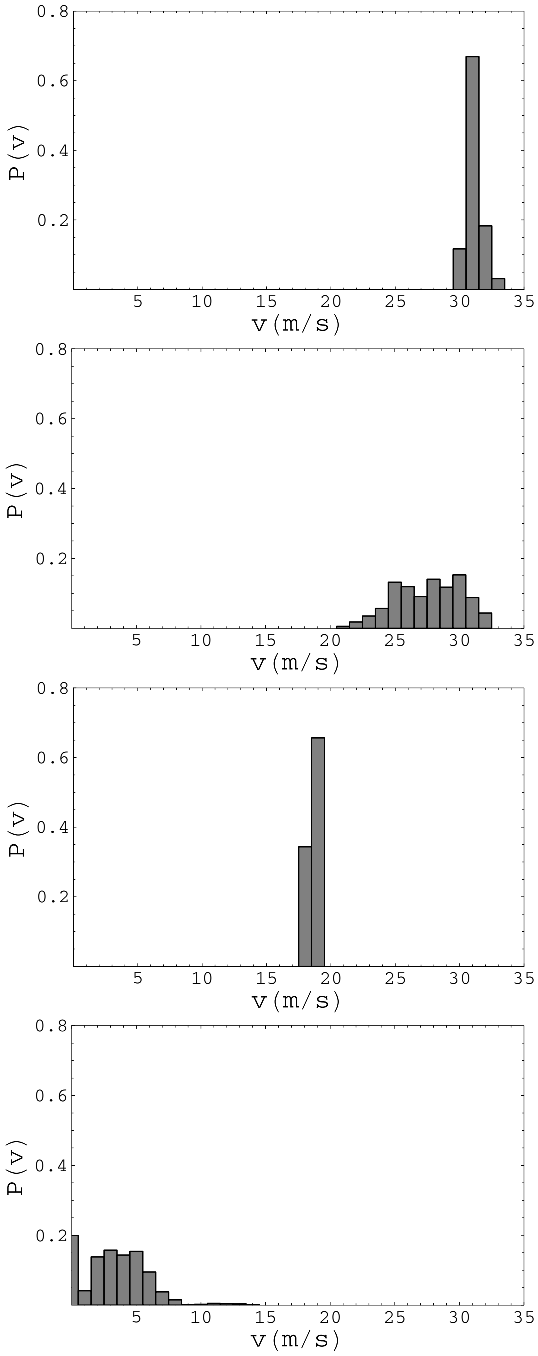

Fig. 5. Single vehicle velocity distribution functions $P(v)$ in different driving states. From top to bottom: F, RF, S and VS driving states.

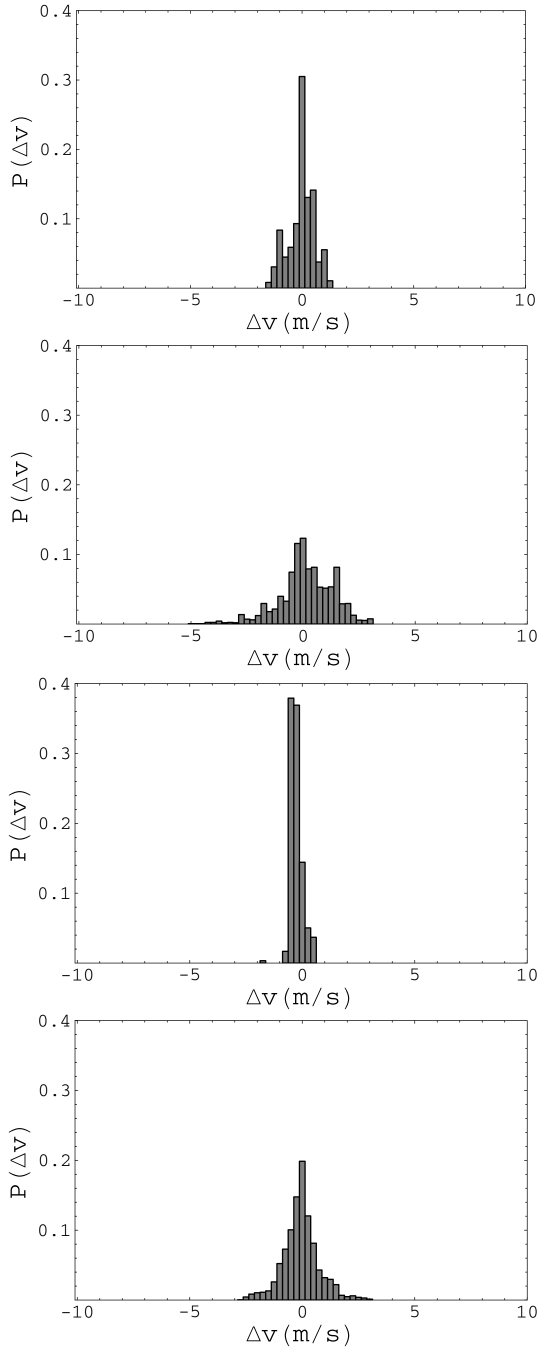

Fig. 6. Single vehicle velocity difference $P(\Delta v)$ distribution functions in different driving states. From top to bottom: F, RF, S and VS driving states.

their domain. This is due to the suppression of fluctuations and could be related to the synchronization of the vehicle's velocity. Finally in the distribution corresponding to the very slow state all $P(v), P(\Delta v)$ and $P(a)$ are widen. We have compared our graph to some of those obtained in fixed detectors. Our gap distribution $P(g)$ in VS state resembles the gap distribution function in congested traffic situation [12].

4.1 Two point distribution functions

Although one point distribution functions give us useful information on quantification of driving behaviours, many important features lie beyond the one point functions and one has to consider higher joint distributions. In this section we present some two-point functions obtained from the empirical data and will discuss their importance for a successful modelling of vehicular dynamic at the microscopic level. Here we show three basic two-point

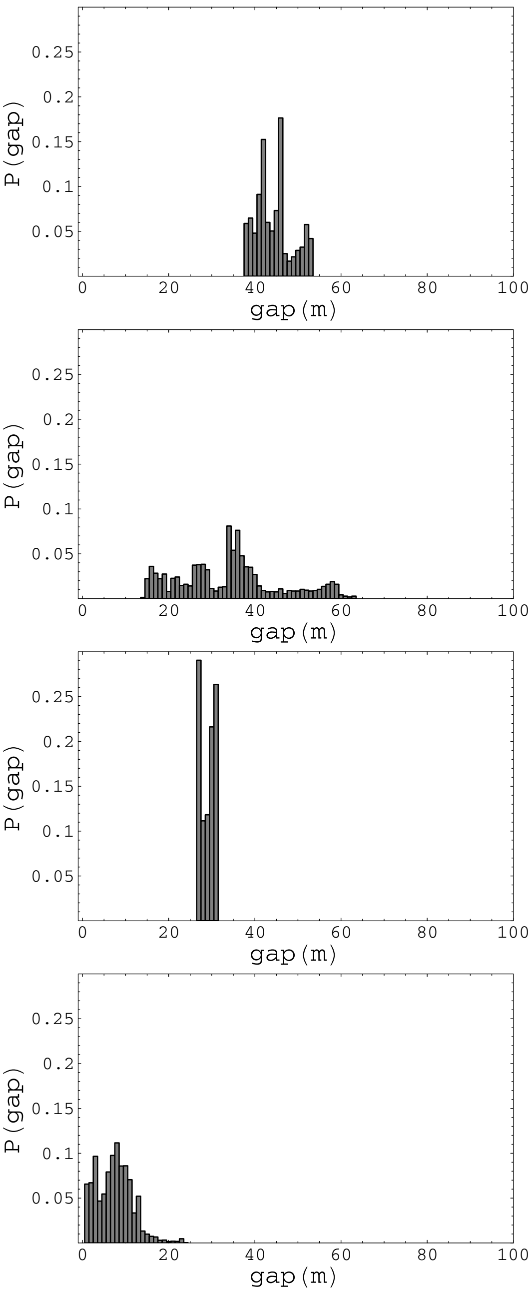

Fig. 7. Single vehicle gap $P(g)$ distribution functions in different driving states. From top to bottom: F, RF, S and VS driving states.

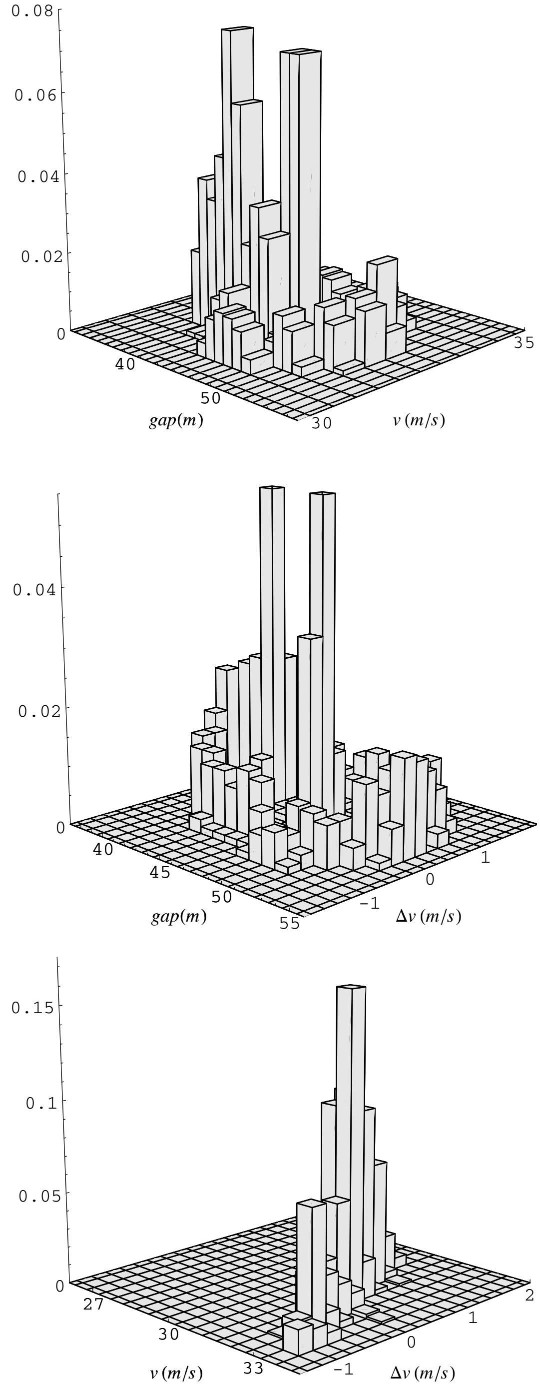

Fig. 8. From top to bottom: $P_2(v, g)$, $P_2(\Delta v, g)$, $P_2(v, \Delta v)$ for a fast (F) drive.

distribution functions, namely $P_2(v, g), P_2(\Delta v, g)$ and $P_2(v, \Delta v)$ for the traffic states discusses so far. The grid values are the same as in one-point functions i.e., velocity grid=1 m/s, velocity difference grid = 0.25 m/s, gap grid = 1 m and acceleration/deceleration grid = 0.1 m/s^2. The number of data points in each bin can simply be evaluated by multiplying the bin's height at the data number of the corresponding driving state.

We shall now investigate, in some details, the characteristics of these distributions. First, let us discuss $P_2(v, g)$. From this distribution we get useful information which relates the velocity to the gap value. According to the free flow graph (Fig. 8), the relative frequencies are scattered in the 2D area. If in the two dimensional $v - g$ plane we mark those grids having large amplitudes in the $P_2(v, g)$, then we can obtain insight on how the gap and velocity are dependent on each other. The same arguments can be applied to $P_2(v, \Delta v)$ and $P_2(\Delta v, g)$.

In the RF driving state, one observes the degree of dependence between velocity and gap has increased at more points. This can be verified by close examination of the diagram. In fact, we notice the number of relatively large columns are increased which consequently gives rise to more marked points in the 2D $g - v$ plane. This implies the optimal velocity assumption can be justified (although not precisely). The optimal velocity curve can be obtained by fitting through the points in $v - g$ plane at which $P_2(v, g)$ has notable values. We have not plotted the two point functions in S state due to insufficient number of data points. Finally in the VS state, the dependence between v and g substantially reduces. This is manifested by looking at the distribution itself and noting the small number of grids having notable value of $P - 2(v, g)$. This may limit the validity of the optimal velocity assumption in this driving state. Nevertheless, we remark the confirmation of this conclusion needs analysis of further data. Next, we discuss the characteristics of $P_2(\Delta v, g)$ in different states. As can be seen by examining the high value grids, in F and RF states, Δv and g are dependent to each at certain points in the 2D $g - \Delta v$ plane. This is suppressed in VS state. Concerning $P_2(v, \Delta v)$, the diagrams tell us that in the fast state, v and Δv are dependent only in a limited curve-like region of the $v - \Delta v$ plane whereas, in RF state, the dependence region appears as 2D area the $v - \Delta v$ plane. By contrast, in the VS state, the dependence region shrinks and appears in a more restricted region of the $v - \Delta v$ plane.

5 Summary and concluding remarks

In this paper we have analysed the floating-car data taken from instrumented vehicles. It has been our emphasis to describe these data on the account of time series analysis. Our findings suggest the existence of four different driving states classified as fast, relatively fast, slow and very slow state. The identification of these states are based on statistical characteristics such as the times series mean, standard deviations, temporal correlation and cross correlation etc. Specifically, we have evaluated the one and two points joint distribution functions. Their analysis has shed light on the *optimal velocity* postulate. Generally speaking, our analysis demonstrates that the degree of validity of the optimal velocity assumption depends on driving state. This gives a rather important hint for the improvement of the car-following approach [33]. In fixed detector data, the O–V curve [12] is somewhat different to the curve obtained from instrumented vehicle. The former is obtained by putting the (v, g) points corresponding to each vehicle passing the fixed detector in the 2D $v - g$ plane while in floating car approach, we put the point (v, g) obtained at each time interval 0.1 s in the 2D $v - g$ plane. Apparently the O–V curve in the optimal velocity model corresponds to the latter case but we remark that one has to average over many floating car data corresponding to many drivers. Knowing the distribution functions, allows us to develop a general framework for modeling of vehicular dynamics. As explained, the diverse types of driver reactions to stimuli received from the traffic ahead of them gives rise to heterogeneous driving strategies. The manifestation of these strategies is reflected in the non-trivial joint distribution functions of driving quantities. This suggests that if we can measure these joint functions in different traffic situations i.e., free, synchronized and congested, then one can make use of them in order to establish a realistic choice of driving strategies by the appropriate designation of acceleration a in terms of v, g and Δv. Let us clarify this point. Apparently we know that the car's acceleration a is related to

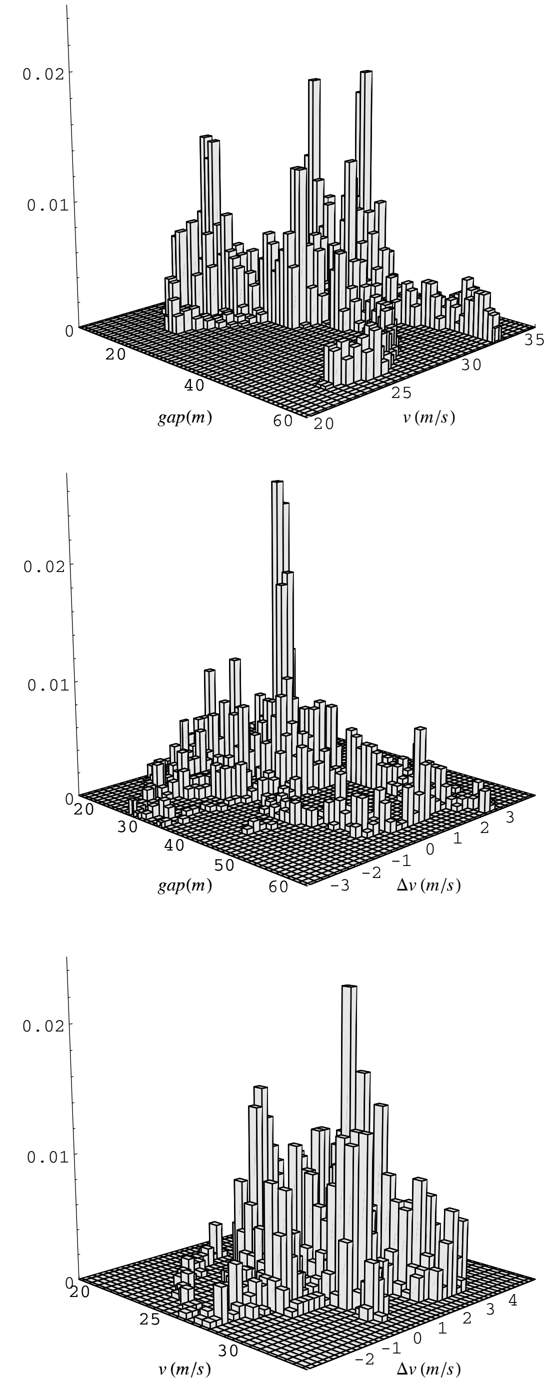

Fig. 9. From top to bottom: $P_2(v, g)$, $P_2(\Delta v, g)$, $P_2(v, \Delta v)$ for a relatively fast (RF) drive.

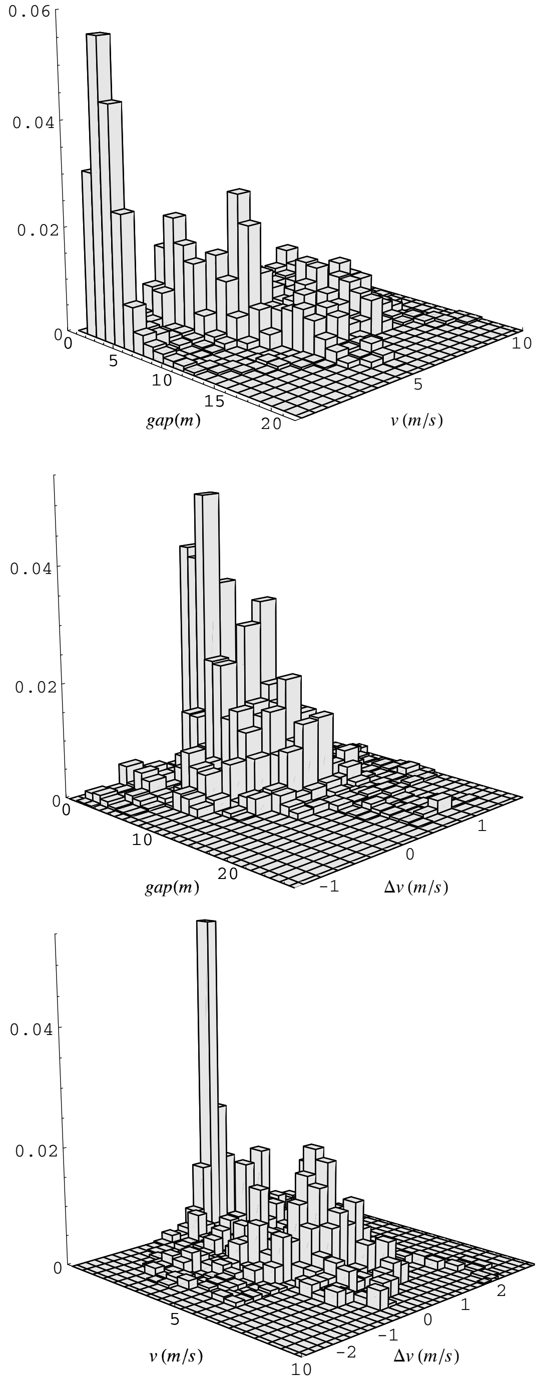

Fig. 10. From top to bottom: $P_2(v, g)$, $P_2(\Delta v, g)$, $P_2(v, \Delta v)$ for a very slow (VS) drive.

its velocity v, its gap g and the velocity difference Δv but we do not know the quantitative relationship. The subtle point is that this relationship is not a functional form in which a is assumed to be a function of v,g and Δv. The empirical data confirms the existence a multitude of acceleration value for fixed values of v, g and Δv. This makes us speak about the probability of having an acceleration value provided the velocity, gap and the velocity difference have values v, g and Δv respectively. The following procedure gives us this conditional probability on a numerical basis. First we evaluate the four and three point functions $P_4(a, g, v, \Delta v)$ and $P_3(g, v, \Delta v)$. Then we proceed by finding the conditional probability that the car's acceleration is a given the velocity, gap and the velocity difference have the values v, g and Δv respectively. This conditional probability is obtained as follows:

$$P(a|g, v, \Delta v) = \frac{P_4(a, g, v, \Delta v)}{P_3(g, v, \Delta v)}. \tag{4}$$

The above conditional probability can be used to model the vehicular dynamics. Details of this approach will be published elsewhere. Moreover, for those car-following models which use a functional dependence of acceleration in terms of v, g and Δv, the above conditional form of the dependence of a in terms of v, g and Δv can be exploited to derive functional form by finding the average value of the acceleration with respect to the above probability distribution as follows:

$$a(g, v, \Delta v) = \sum_a aP(a|g, v, \Delta v). \tag{5}$$

The above procedure can easily be extended to the cases where a is assumed to depend on more variables rather than v, g and Δv. Our next objective is the challenge of finding improved vehicular dynamics which are more advantageous than the existing ones through investigation of distribution functions. Finally, it must be mentioned that our data is related to only a few instrumented cars. In order to draw decisive and exhaustive conclusions, one has to obtain sufficiently large data-set from a variety of drivers. Analysis of future floating-cars data will shed more light upon the problem.

We are deeply indebted to the *Institute of Transport Research (IVF)* at German Aerospace centre (DLR) and in particular Peter Wagner for providing us with the empirical data. The data have been gathered by the Robert Bosch GmbH and are available in the IVF web site [30]. Special thanks is given to Richard W. Sorfleet for his patience in reading the manuscript.

References

1. B. Kerner, in *Physics of Traffic* (Springer, 2004)
2. *Traffic Flow Fundamentals*, edited by A.D. May (Prentice Hall, 1990)
3. *Transportation and Traffic Theory*, edited by C.F Daganzo (Elsevier, 1993)
4. D. Chowdhury, L. Santen, A. Schadschneider, Phys. Rep. **329**, 199 (2000)
5. D. Helbing, Rev. Mod. Phys. **73**, 1067 (2001)
6. B.S. Kerner, Networks and Spatial Economics **1**, 35 (2001)
7. *Traffic and Granular flow*, edited by H.J. Herrmann, D. Helbing, M. Schreckenberg, D.E. Wolf (Springer, Berlin, 2000)
8. *Traffic and Granular flow*, edited by M. Fukui, Y. Sugiyama, M. Schreckenberg, D.E. Wolf (Springer, Tokyo, 2002)

9. B.S. Kerner, Phys. Rev. E **65**, 046138 (2002)
10. I. Lubashevsky, R. Mahnke, P. Wagner, S. Kelenov, Phys. Rev. E **66**, 016117 (2002)
11. L. Neubert, L. Santen, A. Schadschneider, M. Schreckenberg, Phys. Rev. E **60**, 6480 (1999)
12. W. Knospe, L. Santen, A. Schadschneider, M. Schreckenberg, Phys. Rev. E **65**, 056133 (2002)
13. D. Helbing, M. Schreckenberg, Phys. Rev. E **59**, R2505 (1999)
14. M. Treiber, A. Hennecke, D. Helbing, Phys. Rev. E **62**, 1805 (2000)
15. W. Knospe, L. Santen A. Schadschneider, M. Schreckenberg, J. Phys. A: Math. Gen **33**, L477 (2000)
16. B.S. Kerner, S.L Klenov, J. Phys. A **35**, L31 (2002)
17. B.S. Kerner, S.L Klenov, D.E. Wolf, J. Phys. A **35**, 9971 (2002)
18. R. Jiang, Q.S. Wu, J. Phys. A **36**, 381 (2003)
19. K. Nagel, P. Wagner, R. Woesler, Oper. Res. **51** (2003)
20. P. Wagner, e-print `arXiv:cond-mat/0411066`
21. B. Kerner, H. Rehborn, Phys. Rev. E **53**, R1297 (1996); B. Kerner, H. Rehborn, Phys. Rev. E **53**, R4275 (1996)
22. B. Kerner, H. Rehborn, Phys. Rev. Lett. **79**, 4030 (1997); B. Kerner, Phys. Rev. Lett. **81**, 3797 (1998)
23. M. Trieber, A. Henneke, D. Helbing Phys. Rev. E **62**, 1805 (2000)
24. B. Kerner, Phys. Rev. E **65**, 046138-1 (2002)
25. B. Kerner, S.L. Klenov, Phys. Rev. E, **68**, 036130 (2003)
26. W. Knospe, L. Santen, A. Schadschneider, M. Schreckenberg, Phys. Rev. E **70**, 016115 (2004)
27. E.P. Todosiev, L.C. Barabosa, Traffic Engineering **34**, 17 (1963)
28. M. Brackstone, B. Sultan, M. McDonald, Tranp. Res. F **5**, 329 (2002)
29. P. Hidas, P. Wagner, German Aerospace Centre (DLR) preprint 2004
30. The data have been gathered by the Robert Bosch GmbH on the highway A 8 along the route between Stuttgart and Karlsruhe in 1995. The data are available on the web-site: `http://www.clearingstelle-verkehr.de/cs/verkehrsdaten`
31. P. Hidas, Traffic Enginering + Control **39**(5), 300 (1998)
32. G.S. Gurusinghe, T. Nakatsuji, Y. Azuta, P. Ranjitkar, Tanaboriboon Transportation. Res. Board conference 2003, paper no TRB2003-004137 (2003)
33. P. Wagner, I. Lubashevsky, e-print `arXiv:cond-mat/0311192`
34. J.H. Banks, Transportation Research B **37**, 539 (2003)